UNCLASSIFIED

CENTRAL RESEARCH LIBRARY
DOCUMENT COLLECTION

MARTIN MARIETTA ENERGY SYSTEMS LIBRARIES
3 4456 0349905 1

ORNL-2013
Health and Biology

cy. 4

NEUTRON SCATTERING

J. W. Cure, III

CENTRAL RESEARCH LIBRARY
DOCUMENT COLLECTION
LIBRARY LOAN COPY
DO NOT TRANSFER TO ANOTHER PERSON
If you wish someone else to see this document, send in name with document and the library will arrange a loan.

OAK RIDGE NATIONAL LABORATORY
OPERATED BY
UNION CARBIDE NUCLEAR COMPANY
A Division of Union Carbide and Carbon Corporation
UCC
POST OFFICE BOX P • OAK RIDGE, TENNESSEE

UNCLASSIFIED

Cy-4. C. R. Litz

ORNL-2013
ERRATA

UNCLASSIFIED

Page No.	Line	Errata
29	Last Equation	Equation should read:

$$E(K, \pi/2) = \int_0^{\pi/2} \sqrt{1 - K^2 \sin^2 \psi}\, d\psi$$

$$= \frac{\pi}{2}\left[1 - \left(\frac{1}{2}\right)^2 K^2 - \left(\frac{3}{2\cdot 4}\right)^2 \frac{K^4}{3}\right.$$

$$- \left(\frac{3\cdot 5}{2\cdot 4\cdot 6}\right)^2 K^6/5 \text{ - - - - - - - -}$$

Changed 7-13-56

UNCLASSIFIED

ORNL-2013

Copy No. 4

Contract No. W-7405-eng-26

HEALTH PHYSICS DIVISION

NEUTRON SCATTERING

John Wilder Cure, III

DATE ISSUED

DEC 9 1955

Oak Ridge National Laboratory
Operated by
Union Carbide Nuclear Company
A Division of Union Carbide and Carbon Corporation
Post Office Box P
Oak Ridge, Tennessee

UNCLASSIFIED

ORNL-2013
Health and Biology

INTERNAL DISTRIBUTION

1. C. E. Center
2. Biology Library
3. Health Physics Library
4-5. Central Research Library
6. Reactor Experimental Engineering Library
7-18. Laboratory Records Department
19. Laboratory Records, ORNL R.C.
20. A. M. Weinberg
21. L. B. Emlet (K-25)
22. J. P. Murray (Y-12)
23. J. A. Swartout
24. E. H. Taylor
25. E. D. Shipley
26. K. Z. Morgan
27. F. C. VonderLage
28. W. H. Jordan
29. S. J. Cromer
30. C. P. Keim
31. J. H. Frye, Jr.
32. R. S. Livingston
33. S. C. Lind
34. F. L. Culler
35. A. H. Snell
36. A. Hollaender
37. M. T. Kelley
38. T. A. Lincoln
39. A. S. Householder
40. C. S. Harrill
41. C. E. Winters
42. D. W. Cardwell
43. J. A. Lane
44. E. E. Anderson
45. D. D. Cowen
46. R. A. Charpie
47. C. E. Clifford
48. M. J. Skinner
49. R. R. Dickison
50. G. S. Hurst
51. H. P. Yockey
52. R. H. Ritchie
53. R. D. Birkhoff
54. M. Slater
55. J. A. Auxier
56. J. Neufeld
57. K. M. Henry
58. F. M. Glass
59. E. P. Blizard
60. F. C. Maienschein
61. ORNL Document Reference Library, Y-12 Branch

EXTERNAL DISTRIBUTION

62. R. F. Bacher, California Institute of Technology
63. G. E. Thoma, USAF
64. T. A. Barr, Physics Department, University of Georgia
65. M. S. Plesset, California Institute of Technology
66. R. G. Cochran, Pennsylvania State College, State College, Pa.
67. R. S. Burington, 1834 N. Hartford St., Arlington, Virginia
68-72. J. W. Cure, III, 37 Perimeter Drive, SE, Albuquerque, New Mexico
73. Division of Research and Medicine, AEC, ORO
74-401. Given distribution as shown in TID-4500 under Health and Biology category

DISTRIBUTION PAGE TO BE REMOVED IF REPORT IS GIVEN PUBLIC DISTRIBUTION

MARTIN MARIETTA ENERGY SYSTEMS LIBRARIES
3 4456 0349905 1

TABLE OF CONTENTS

I. Introduction 1

II. Experimental Arrangement and Equipment 3

III. Check and Calibration 8

IV. Experimental Data 10

V. Theory 17

VI. Conclusion 22

Appendix I 23

Bibliography 34

LIST OF FIGURES

1. Experimental arrangement for scattering of fast neutrons 4

2. Block diagram of electronic equipment 5

3. Diagram of proportional counter tube 6

4. Dose rate variation vs h for 20 cm from center of source to center of detector 11

5. Dose rate variation vs h for 40 cm from center of source to center of detector 11

6. Dose rate variation vs h for 80 cm from center of source to center of detector 12

7. Dose rate variation vs h for 160 cm from center of source to center of detector 12

8. Dose rate variation vs h for 240 cm from center of source to center of detector 13

9. Dose rate variation vs h for 320 cm from center of source to center of detector 13

10. Dose rate variation vs h for 80 cm from center of source to center of detector with a 44 cm paraffin frustum between the source and detector 15

11. Dose rate variation vs h for 160 cm from center of source to center of detector with a 44 cm paraffin frustum between the source and detector 15

12. Comparison of the measured dose and the dose as calculated by the inverse square law 16

13. Comparison between the theoretical curve and the experimental data 20

14. Geometry for scattering 24

15. Function f(k) vs k 32

ABSTRACT

Scattered radiation reaching the point of measurement is one of the major problems of neutron dosimetry. An experiment was designed to determine the variation in neutron dose rate at a point in air with, (a) the distance between the source and the detector, and (b) the height of the source and detector above a concrete slab.

The experimental data are compared with data obtained from the albedo theory, and the results agree within the experimental error. When a conical frustum of paraffin, which reduces the direct beam of neutrons by a factor of a few thousand, was placed between the source and detector, only the scattered neutrons contributed to the dose rate. This method gives data which enables one to correct for scattered radiation. To reduce extraneous scattering material to a minimum the detector and source were supported five feet below a steel bar which was suspended from two painter's scaffolds forty feet apart and fifty-five feet high. The neutron source was Polonium-Boron (which gave neutrons with an average energy of 2.5 Mev). The dosimeter was a proportional counter, ethylene-polyethylene type, with a pulse integrator for measuring the tissue dose.

It was found that the inverse square law predicts the dose rate for distances up to approximately 1.5 meters between the source and the detector; and if the source, detector, etc. are 1.5 meters from the walls, floor, etc., the dose rate contribution at the detector due to scattered neutrons is less than six per cent. The results of this experiment apply directly to the calibration of a neutron dosimeter in air.

I. INTRODUCTION

The purpose of this experiment was to test the theories of neutron scattering and to improve the technique of neutron dosimetry. Scattered radiation reaching the point of measurement is one of the major problems in neutron dosimetry because it increases the dose rate above that predicted by the inverse square law. An instrument calibrated at a point where appreciable scattered neutrons were present would give an erroneously low reading in the field where the instrument would be used. If the dose rate due to scattered neutrons were known, the calibration could be corrected accordingly.

One can experimentally observe the variation in neutron dose rate at a point in air, as a function of the distance between the source and the detector. This variation in dose rate can be compared with values of neutron dose rate calculated using the inverse square law. Also, one can experimentally observe the variation in neutron dose rate as a function of the height of the source and detector above a concrete slab. If a conical frustum of paraffin is interposed between the source and the detector, one can measure the scattered neutron dose rate as a function of the height of the source and detector above the concrete slab. These measurements can be compared with values obtained from theoretical considerations.

The detector used was an ethylene-polyethylene neutron dosimeter.

This instrument is essentially non-directional,[1] i.e., its response is independent of the angle of incident of the neutrons.

The subject matter of this thesis has been reported.[2]

---

[1] Barr, T. A., and Hurst, G. S., Nucleonics 12, No. 8, 33 (August 1954).

[2] Cure, J. W., and Hurst, G. S., Nucleonics 12, No. 8, 36 (August 1954).

II. EXPERIMENTAL ARRANGEMENT AND EQUIPMENT

The experimental arrangement is shown in Fig. 1. The towers are of the painter's scaffold type. The steel bar, suspended between the two towers by steel cables, can be raised and lowered by hoists. The detector and source are held approximately 1.5 meters below the bar by aluminum rods. Two steel measuring tapes, one at each end of the bar, assure that the source and detector are always at the same height above the concrete. The thickness of the concrete slab varied from three to four inches.

The electronic equipment is shown in the block diagram of Fig. 2. The ethylene-polyethylene detector,[3] which operates as a proportional counter, is shown in Fig. 3. It is filled with ethylene to approximately one atmosphere of pressure and is lined with polyethylene. The detector is rigidly fixed to the preamplifier with an amphenol coaxial connector. The preamplifier, detector, and a desiccant ("Drierite") were put into a polyethylene bag one mil thick, and the bag was sealed. The polyethylene bag had no detectable effect on the dose rate. The sealed bag was necessary because it prevented the noise level of the detector from rising to a prohibitively high level due to high humidity. The preamplifier was a cathode follower. A sixty-foot cable connected the preamplifier to the electronic equipment which was in the shed at the rear of one of the towers.

---

[3] Hurst, G. S., and Ritchie, R. H., Radiology, 60, No. 6, 864 (June 1953).

UNCLASSIFIED
ORNL-LR-DWG. 10477

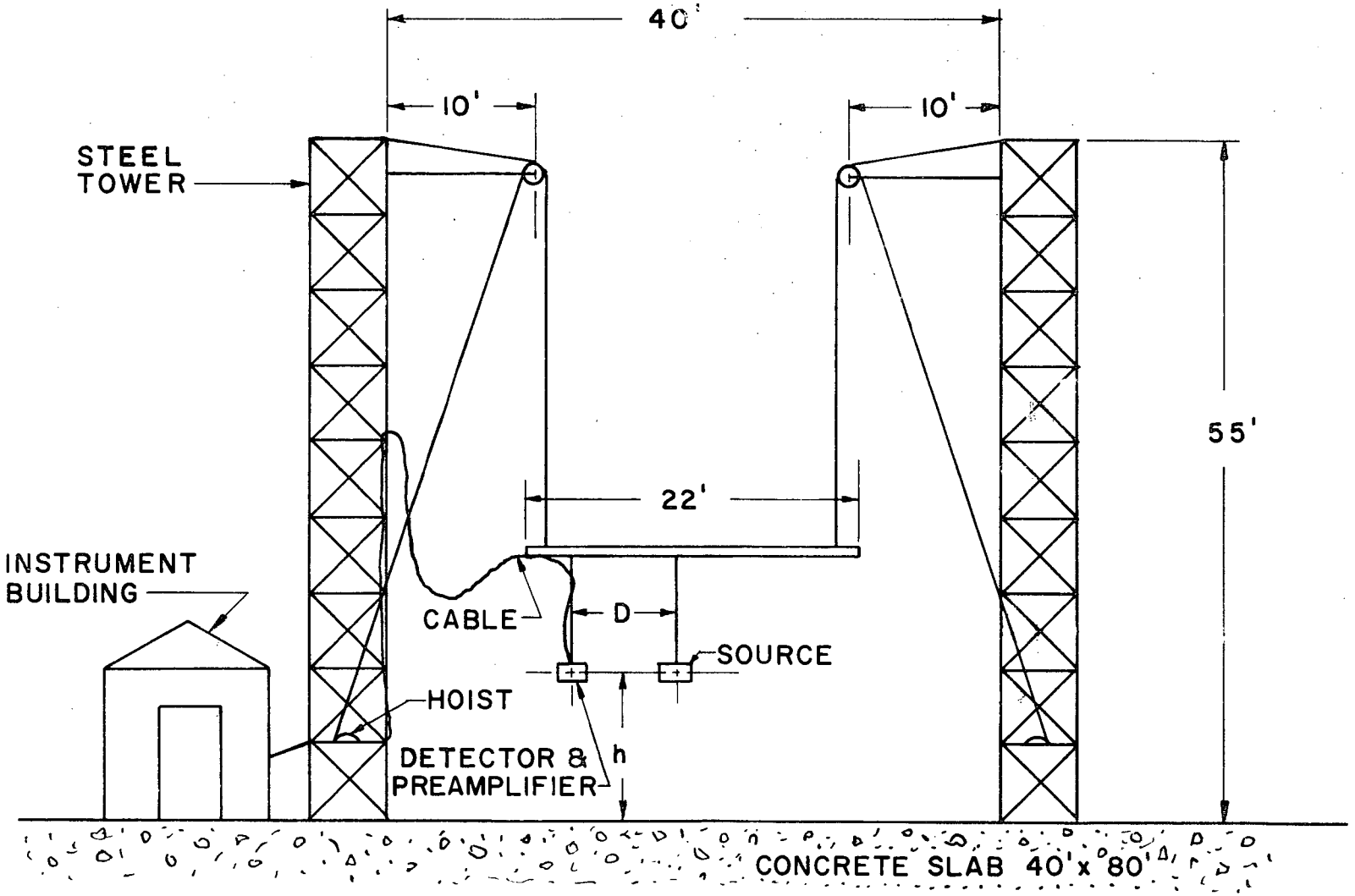

EXPERIMENTAL ARRANGEMENT FOR SCATTERING OF FAST NEUTRONS

FIGURE 1

UNCLASSIFIED
ORNL-LR-DWG. 10478

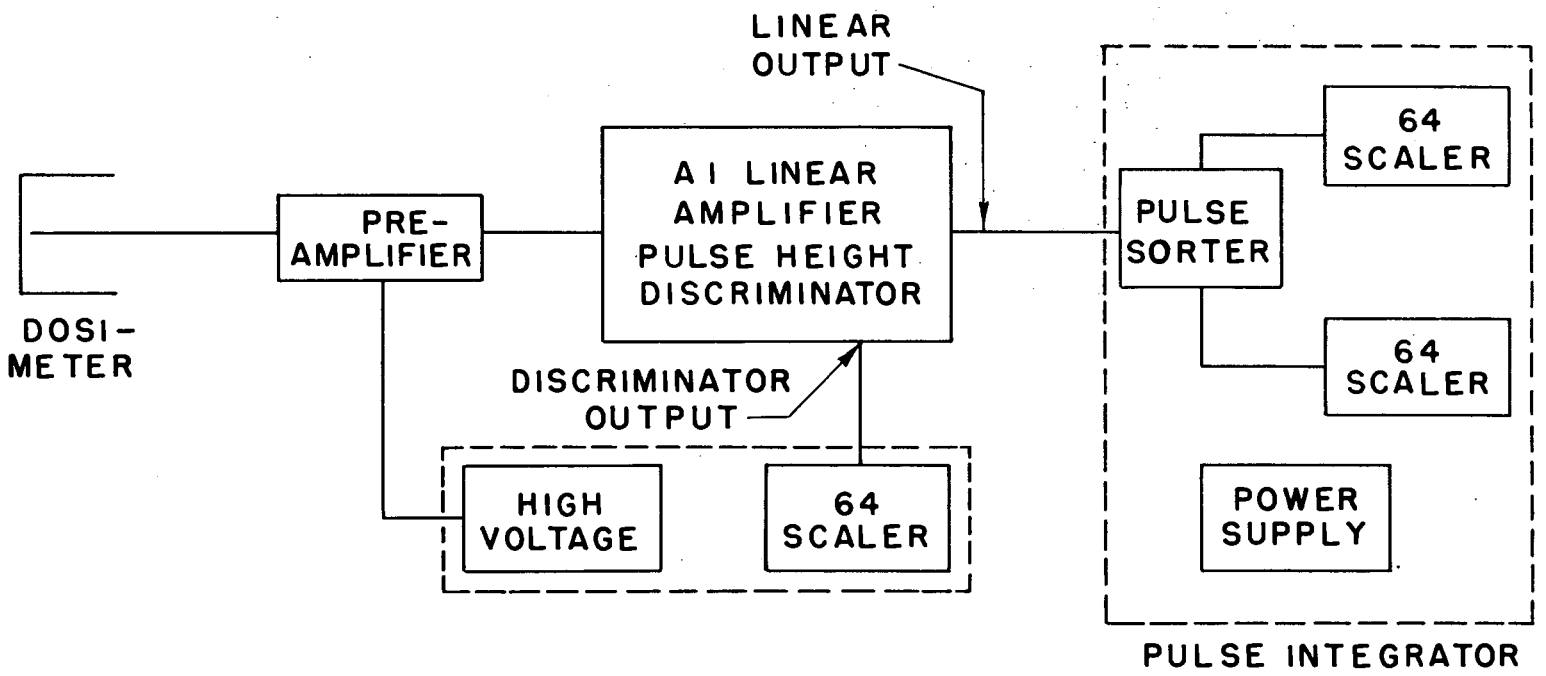

BLOCK DIAGRAM OF ELECTRONIC EQUIPMENT
FIGURE 2

UNCLASSIFIED
ORNL-LR-DWG. 471

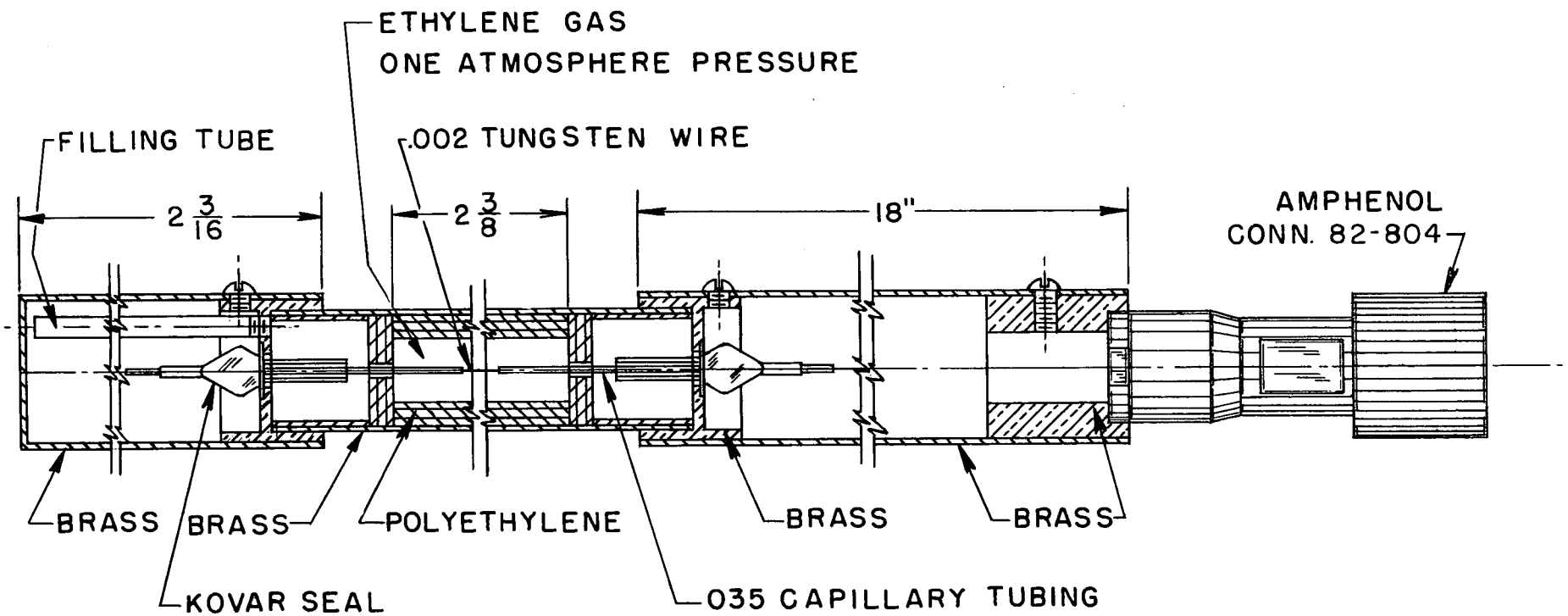

SCALE: 1" = 1"

FIGURE 3

The device which automatically adds the pulse heights is known as a "pulse integrator".[4] It consists of two scales of 64 binary scaling units with a set of discriminators. The set of discriminators is arranged so that all pulses greater than five volts fire indicator "1", ten volts fire indicator "2", twenty volts fire indicator "4", etc. This gives a device which automatically adds pulse heights. In actual operation a five-volt pulse would fire indicator "1". A ten-volt pulse would fire indicator "2". Indicator "1" is fired by this ten-volt pulse if it is in the "off" position, which gives a total of three counts. If indicator "1" is in the "on" position when the ten-volt pulse arrives, it is effectively erased because the second stage is already busy. Thus the effect is to alternately add and subtract a count which gives a net result of two counts per ten-volt pulse on the average. Similar reasoning shows that a twenty-volt pulse gives an average of four counts, a forty-volt pulse gives an average of eight counts, etc. This type of arrangement is extremely simple since there is no need to use anticoincident circuits to prevent additions of pulses from lower level discriminators.

The neutron source used was polonium-boron which gives neutrons with an average energy of 2.5 Mev.[5]

---

[4] Glass, F. M., and Hurst, G. S., Rev. Scient. Instr. 23, No. 2, 67 (February 1952).

[5] Cochran, R. G., and Henry, K. M., ORNL-1479 (April 2, 1953).

III. CHECK AND CALIBRATION

The following checks were made. A calibrated sixty cycle variable pulse height pulser ("Q" pulser), was used to ascertain that the Al amplifier was linear, and it was also used to set the discriminator voltages. The operating voltage of the detector which would effectively cut off gamma pulses was determined. For this purpose the proportional counter tube was placed in a 2 r/hr gamma-ray field (from a Co^{60} source), then the discriminator on the linear Al amplifier was set to six volts which was well above the noise level of the equipment. The high voltage was adjusted to give a gamma response of approximately one pulse per second. The tube had a very sharp gamma cut off. If the Al amplifier discriminator was raised to about nine volts at the same high voltage setting the gamma pulses would be completely cut off. This gamma bias was checked about once a week, and if it had changed, the high voltage was adjusted to again give one pulse per second. Normally the high voltage had to be raised a few volts a week. This changed the neutron dose rate sensitivity. Thus, a standard geometry had to be arranged that could be reproduced from day to day to determine the relative neutron dose rate sensitivity. With this information the dose rate can be converted to a normalized value, and data can at any time be reproduced within the experimental error. The half life of Po^{210} is 138 days; the dose rate was corrected accordingly.

The experimental arrangement was checked to ascertain if there was any detectable neutron scattering from any of the equipment (shed,

towers, bar, etc.). None could be measured.

The high voltage for the detector was monitored with a Leeds and Northrup Potentiometer, so that it could be kept at a particular setting within a tenth of one per cent.

IV. EXPERIMENTAL DATA

Curves showing the dose rate as a function of the distance (h) above the concrete for several different source-to-detector distances (D) are shown in Figs. 4 through 9. This dose rate includes neutrons which travel directly from the source to the detector as well as neutrons that are scattered from the concrete. The dose rate has been normalized to a value of one (one is the dose rate due to direct neutrons) for the flat portion of each curve, and all of the curves have been plotted to the same scale.

As the source and detector approach the concrete from above, for any particular distance (D) between the source and detector, there is a point at which the neutrons scattered from the concrete begin to contribute noticeably to the dose rate. As h decreases further, the number of scattered neutrons reaching the detector increases; therefore there is a rise in the curve. As shown by Figs. 7, 8, 9 and 13, the dose rate reaches a maximum at the point $h/D \cong 0.25$. For smaller values of h/D the neutrons that are scattered have to travel increasingly greater distances through the concrete in order to reach the detector. This results in a net decrease in the dose rate. When $h/D \cong 0.05$, the concrete effectively absorbs the neutrons which would be scattered from the concrete as far as the detector can tell. The dose rate when $h/D \lesssim 0.05$ could possibly be less than the flat portion of the curve because there is 2π air scattering instead of 4π air scattering. The relative deviation (R.D. = $1/\sqrt{N}$) of each count is shown on these curves.

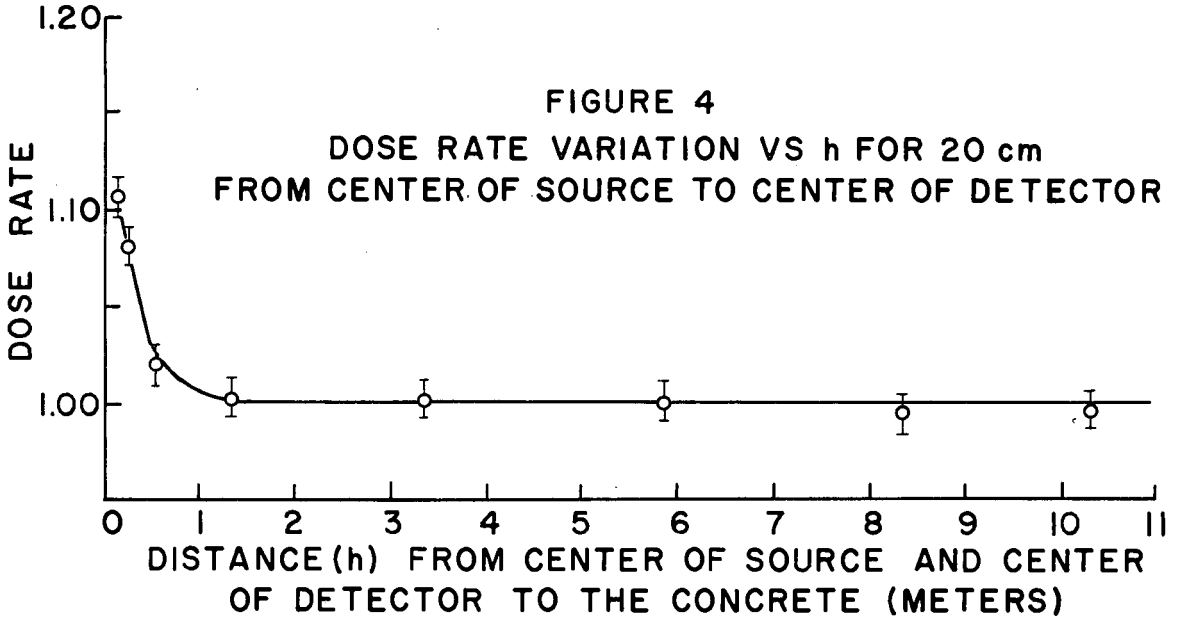

FIGURE 4
DOSE RATE VARIATION VS h FOR 20 cm
FROM CENTER OF SOURCE TO CENTER OF DETECTOR

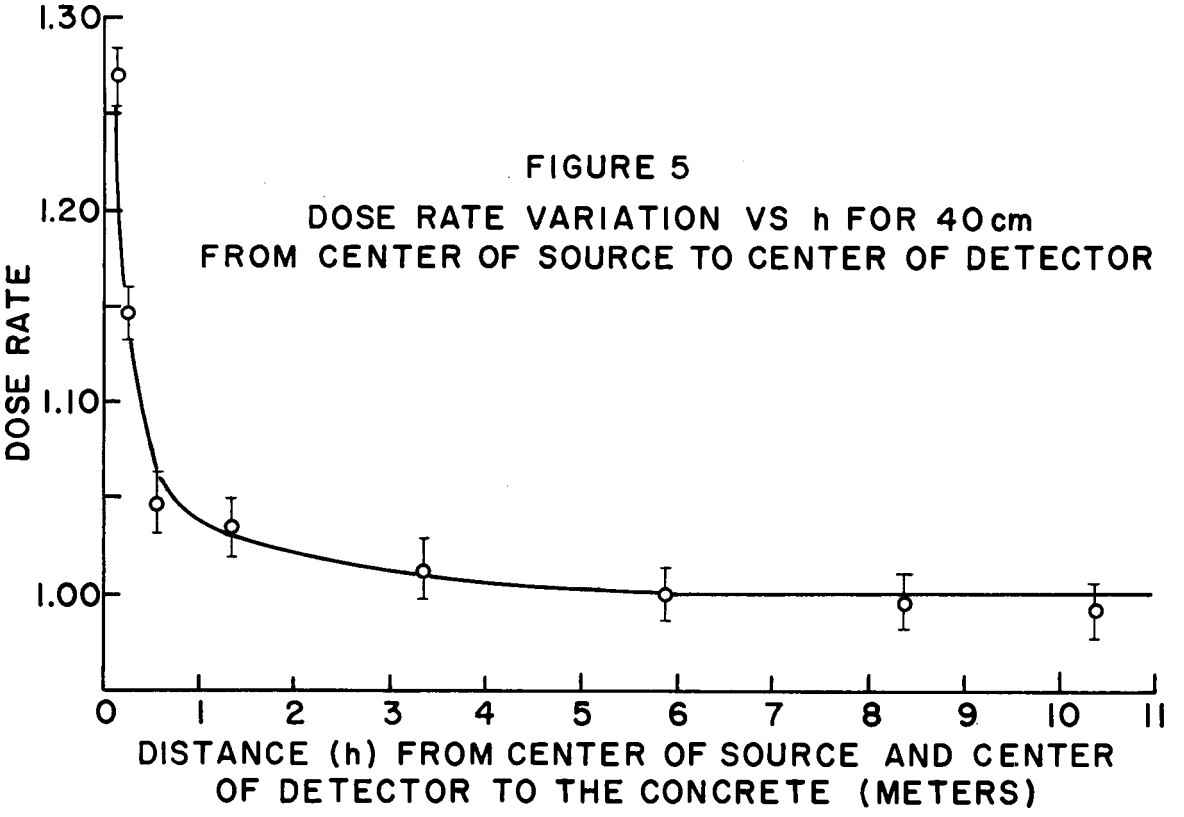

FIGURE 5
DOSE RATE VARIATION VS h FOR 40 cm
FROM CENTER OF SOURCE TO CENTER OF DETECTOR

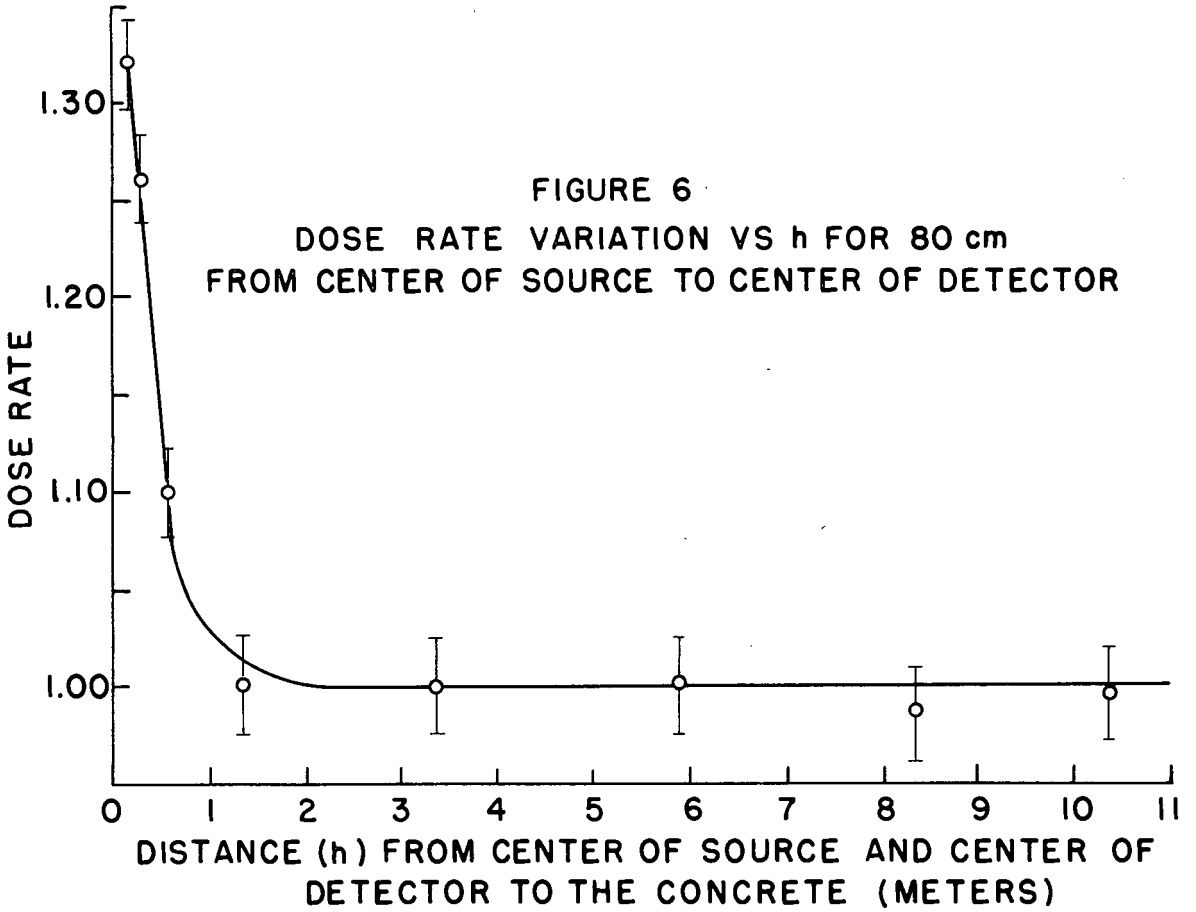

FIGURE 6
DOSE RATE VARIATION VS h FOR 80 cm
FROM CENTER OF SOURCE TO CENTER OF DETECTOR

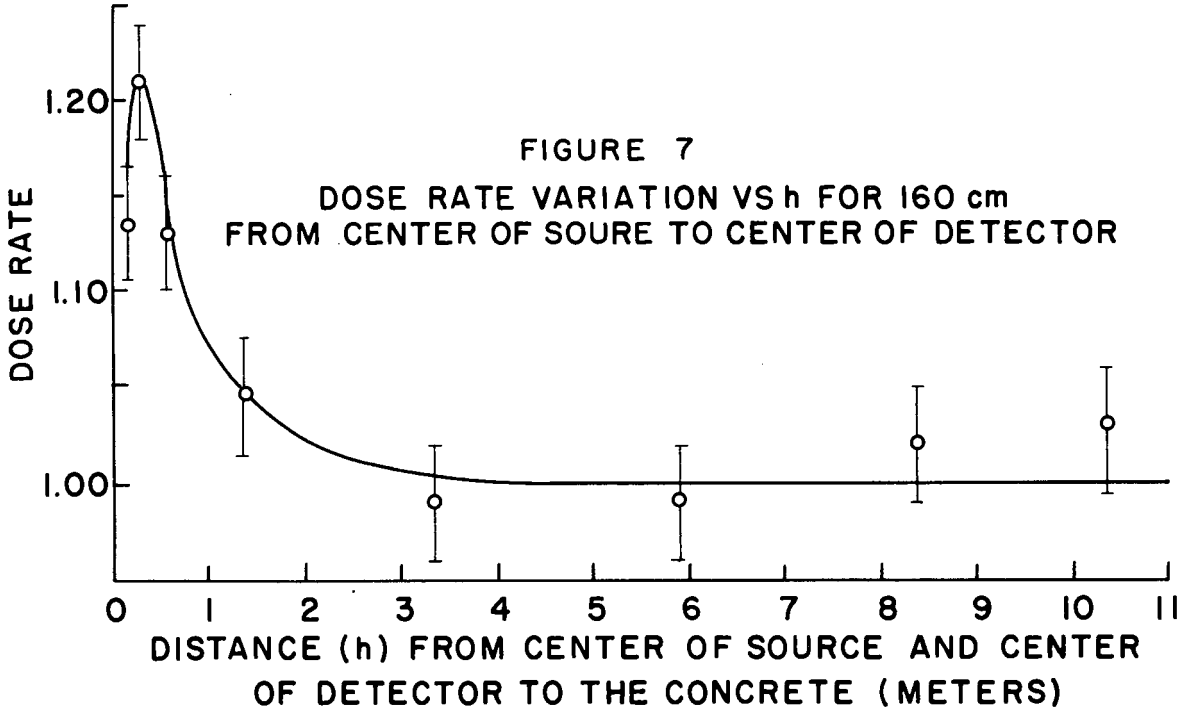

FIGURE 7
DOSE RATE VARIATION VS h FOR 160 cm
FROM CENTER OF SOURE TO CENTER OF DETECTOR

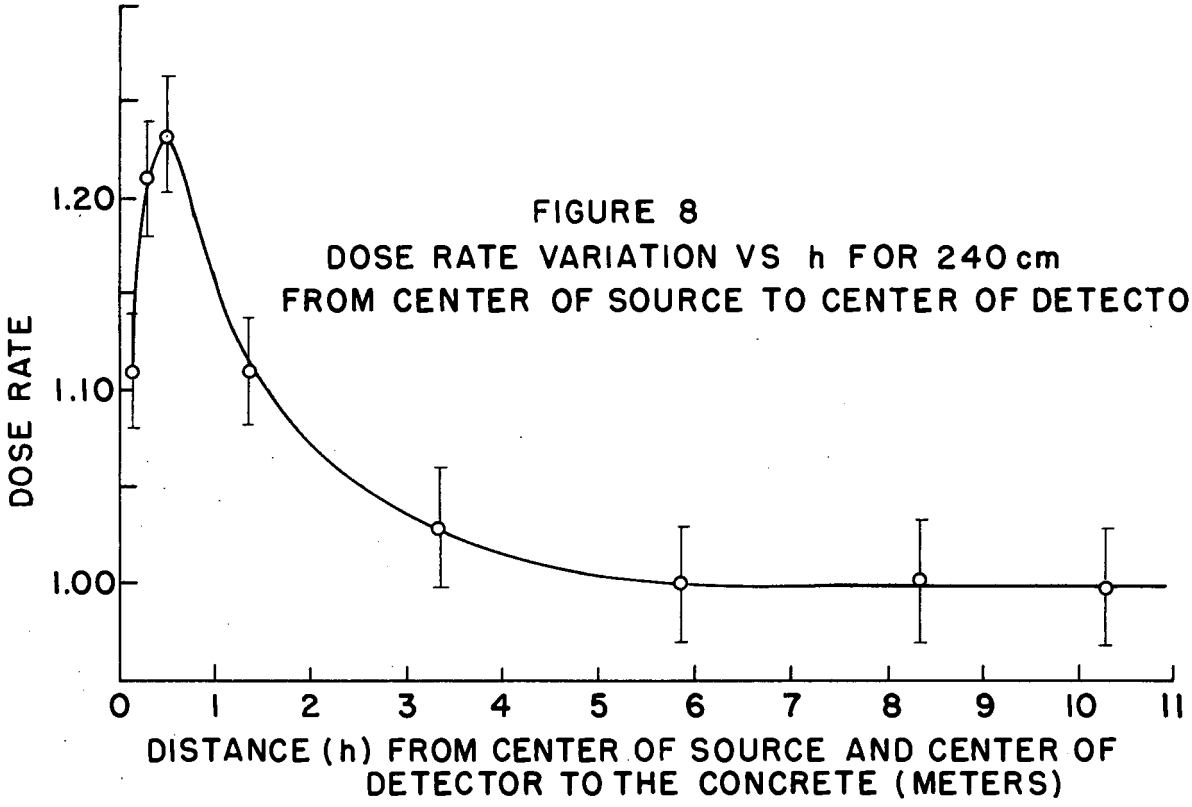

FIGURE 8
DOSE RATE VARIATION VS h FOR 240 cm
FROM CENTER OF SOURCE TO CENTER OF DETECTOR

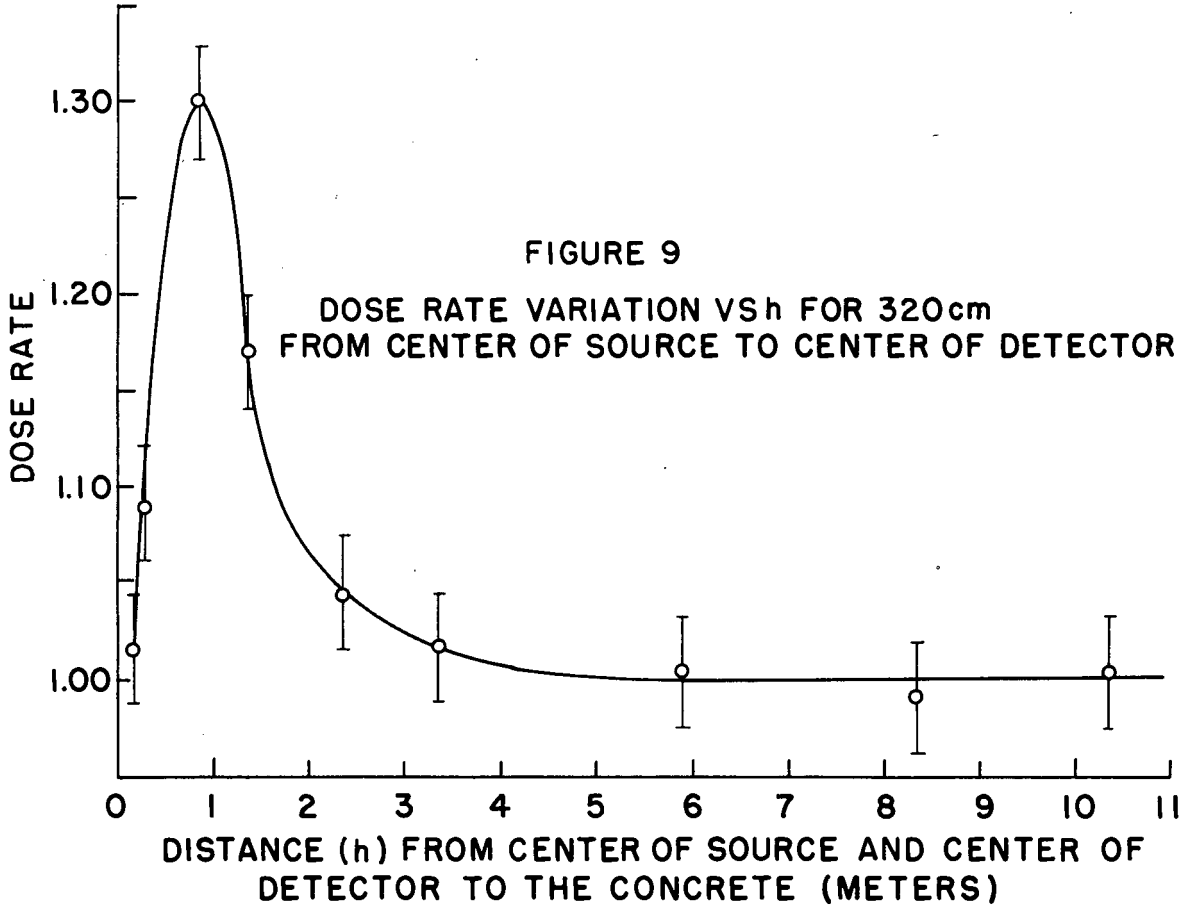

FIGURE 9
DOSE RATE VARIATION VS h FOR 320 cm
FROM CENTER OF SOURCE TO CENTER OF DETECTOR

Figures 10 and 11 are plots of the dose rate against the height of the detector and the source above the surface of the concrete for 80 centimeters and 160 centimeters between the source and detector with a 44-centimeter conical paraffin frustum between the source and detector. The 44 centimeters of paraffin reduced the dose rate of the direct beam by a factor greater than five thousand. These curves follow very closely the portions of the curves of Figs. 7 and 8 due to scatter. Therefore, if a paraffin frustum of sufficient thickness is placed between the source and detector, the dose rate recorded is due to the scattered neutrons only. The relative deviation of each point on these curves is five per cent or less.

Figure 12 is a plot of the dose rate as read from the flat portions of the curves of Figs. 4 through 9, i.e., for heights above the concrete where neutron scattering from the concrete is negligible, against the corresponding distance between the source and the detector. The experimental error of ten per cent is shown on this curve. The dose rate follows the inverse square law up to a distance of about 1.5 meters between the source and detector. Then the dose rate increases above that predicted by the inverse square law. It is thought that this increase above the inverse square law is due to scattering of neutrons by air.

All statistical errors were kept below five per cent. However, other errors (changes in geometry, instrument errors, etc.) may be additive and could make the over-all error as large as ten per cent in some instances.

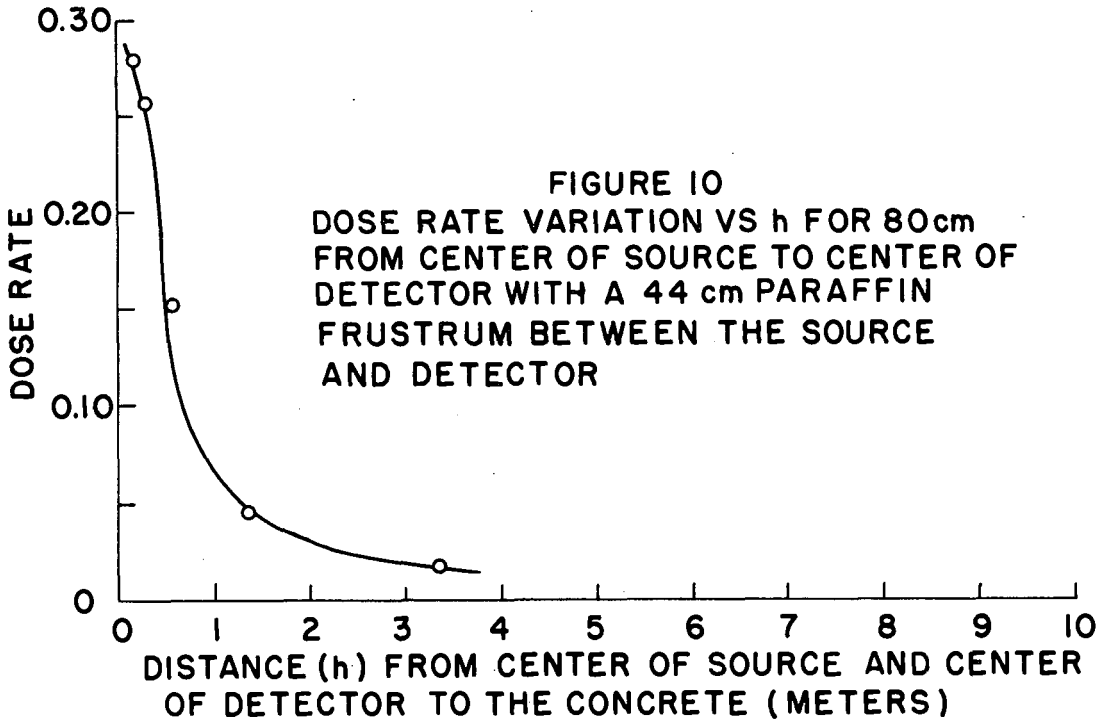

FIGURE 10
DOSE RATE VARIATION VS h FOR 80cm FROM CENTER OF SOURCE TO CENTER OF DETECTOR WITH A 44 cm PARAFFIN FRUSTRUM BETWEEN THE SOURCE AND DETECTOR

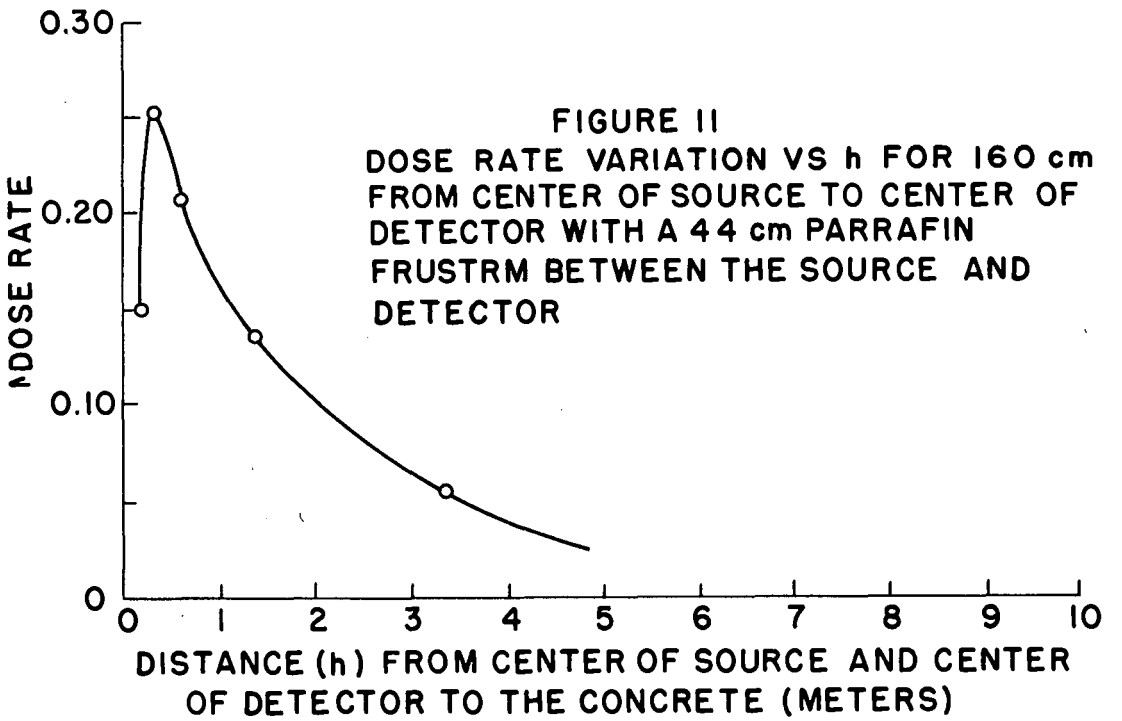

FIGURE 11
DOSE RATE VARIATION VS h FOR 160 cm FROM CENTER OF SOURCE TO CENTER OF DETECTOR WITH A 44 cm PARRAFIN FRUSTRM BETWEEN THE SOURCE AND DETECTOR

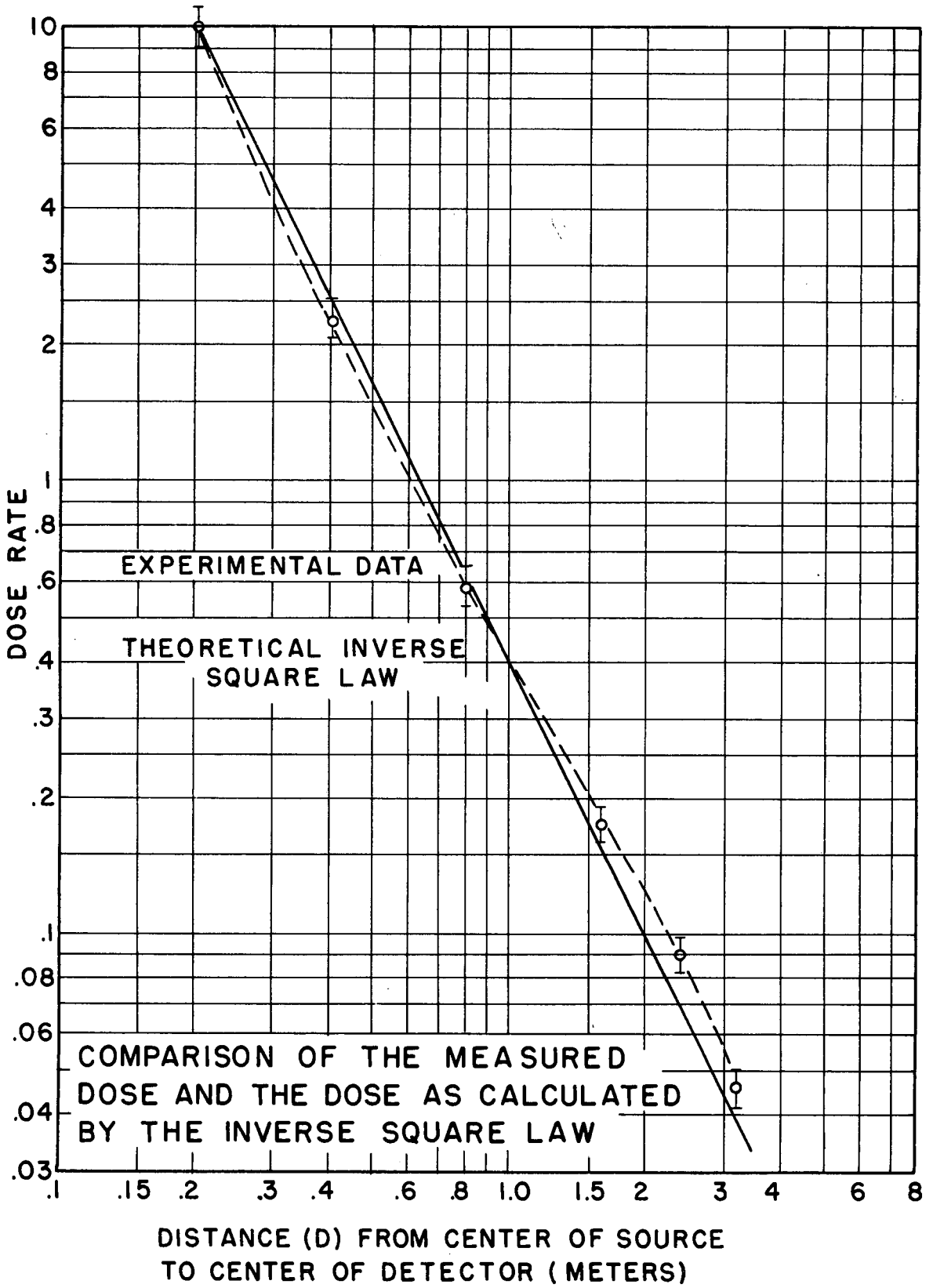
10
8
6
4
3
2
1
.8
.6
.4
.3
.2
.1
.08
.06
.04
.03
DOSE RATE
EXPERIMENTAL DATA
THEORETICAL INVERSE
SQUARE LAW
COMPARISON OF THE MEASURED
DOSE AND THE DOSE AS CALCULATED
BY THE INVERSE SQUARE LAW
.1
.15
.2
.3
.4
.6
.8
1.0
1.5
2
3
4
6
8
DISTANCE (D) FROM CENTER OF SOURCE
TO CENTER OF DETECTOR (METERS)

FIGURE 12

V. THEORY

The proportional counter tube is lined with a layer of polyethylene whose thickness is just greater than the range of the most energetic proton that is produced by PoB neutron collision with hydrogen atoms. The energy dissipated by the recoil protons is proportional to the energy dissipated by the neutrons. The total ionization produced in the detector cavity is proportional to the energy dissipated per gram of ethylene, provided "W" (electron volts/ion pair) is independent of proton energy. If one calculates the first collision dose for neutrons as a function of energy for both tissue and ethylene, one finds that the ratio (ethylene dose/ tissue dose) is essentially independent of neutron energy.[3] This means that the neutron dose delivered to ethylene is proportional to the dose delivered to tissue.

A direct current (dc) measurement of the number of ions produced in the ethylene would be a satisfactory method for determining the dose except for the fact that the measurement would be affected by gamma radiation. To make the instrument insensitive to gamma rays, we use a bias such that the smaller gamma-ray pulses are not counted. Then we determine the number of ion pairs produced by adding the pulse heights. The bias causes some loss of neutron dose, but this is of little significance as long as the neutron energy is greater than 500 kev.[3] The pulse

height is proportional to the number of ion pairs if there is no appreciable electron recombination, and if the Al linear amplifier time constant is made much longer than the time of collection of the electrons.

An absolute neutron tissue dose calibration involves several factors. Either the source strength or the detector dose sensitivity must be known. If the source strength is known, which is the usual case, one can set the detector at some distance from the source, and calculate the neutron flux at the detector by the inverse square law. The equipment should be sufficiently far away from the floors, walls, etc. so that no scattered neutrons are detected. The average dose in reps (1 rep = 93 ergs/gram of tissue) for $Po^{210}B$ neutrons is 3.54×10^{-9} rep - cm^2/neutron.[6] Assuming a neutron source strength of 10^6 n/sec and a source-to-detector distance of 20 centimeters, the neutron flux at the detector is

$$F_n = \frac{N_o}{4\pi D^2} = \frac{10^6 \text{ n/sec}}{4\pi(20)^2 \text{ cm}^2} = 1.99 \times 10^2 \text{ n/cm}^2 \text{ sec.}$$

The neutron dose rate at the detector is

$$\text{Dose Rate} = (1.99 \times 10^2 \text{ n/cm}^2 \text{ sec})(3.54 \times 10^{-9} \text{ rep cm}^2/\text{n})$$

$$\text{Dose Rate} = 7.01 \times 10^{-7} \text{ rep/sec.}$$

---

6 Hurst, G. S., Brit. J. Radiol. XXVII, No. 318, 353 (June 1954).

If the pulse integrator records a dose rate of 200 counts/sec at this distance, the dose sensitivity of the detector is

$$\text{Dose Sensitivity} = \frac{7.01 \times 10^{-7} \text{ rep/sec}}{200 \text{ counts/sec}} = 3.5 \times 10^{-9} \text{ rep/count.}$$

To find the tissue dose the count as recorded on the pulse integrator is multiplied by the dose sensitivity (in this case, 3.5×10^{-9} rep/count).

By means of the albedo theory[7] a theoretical curve can be drawn that agrees with the experimental curve to within the experimental error. The theoretical curve is based on the assumption that the neutrons are scattered from the concrete according to the cosine law.

Taking equation (7) from Appendix I we have,

$$\text{Ratio of Dose Rate} = 1 + \frac{\alpha}{2\pi} k^2 f(k).$$

If this equation is plotted against $1/k$ for comparison with the experimental data (see Fig. 13) then α, the dose albedo, is determined to be approximately 0.32. As can be noted from Fig. 13 the theoretical curve does not fall exactly on the experimental curve, but it is within the experimental error of ten per cent. The theoretical curve lies within the experimental error of the experimental points for the paraffin frustum between the source and detector, except in two cases. These two points are shown

---

[7] Plesset, M. S., RAD-196 (August 1948).

UNCLASSIFIED
ORNL-LR-DWG. 10485

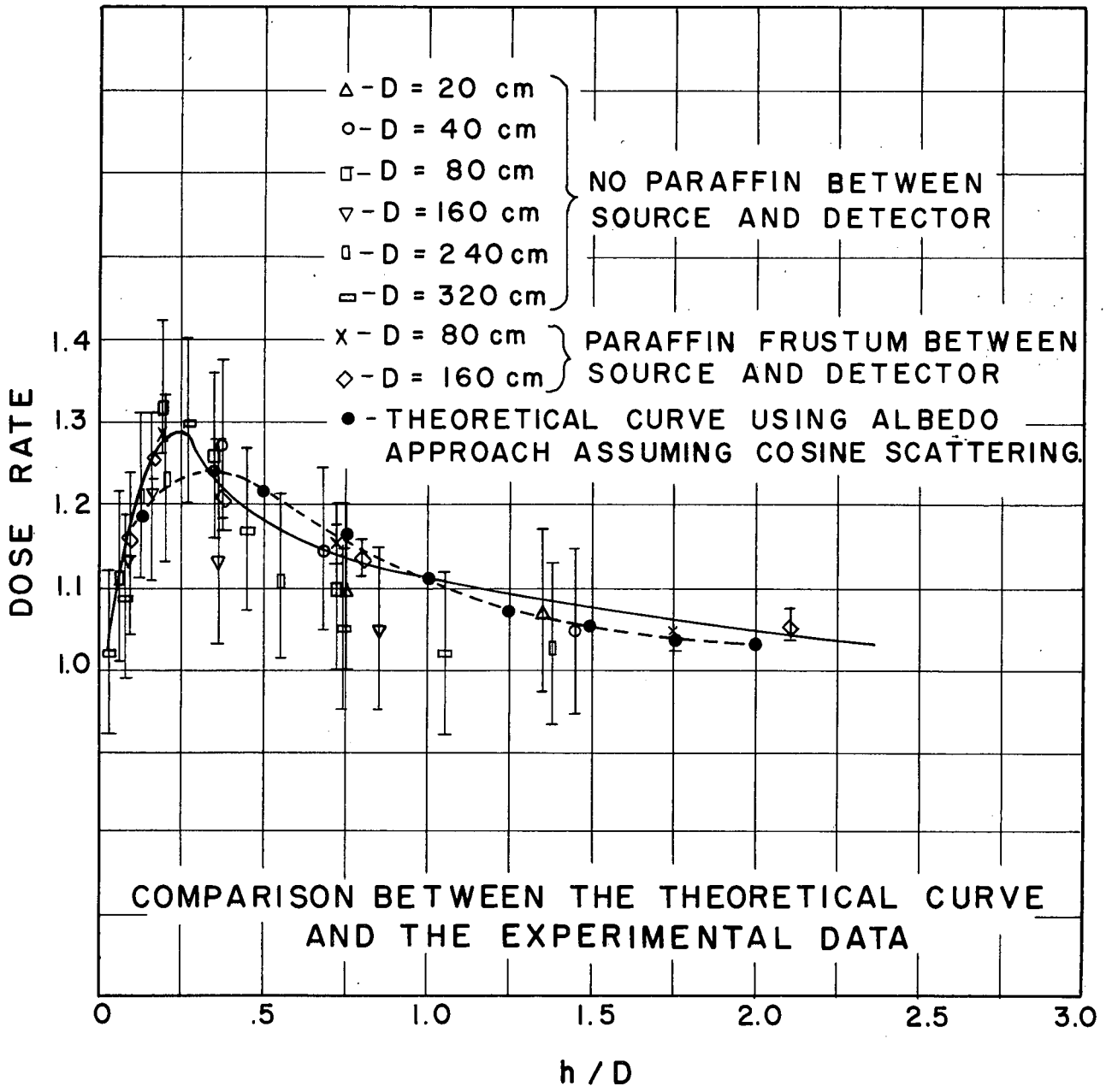

COMPARISON BETWEEN THE THEORETICAL CURVE AND THE EXPERIMENTAL DATA

FIGURE 13

circled in red on Fig. 13. It should be noted that these two points are due to scattered neutrons only and as a result ten per cent error of their value is much smaller than it would be for the points that have the dose rate due to direct neutrons included. The only two points which did not fall on the theoretical curve are the two points for $h/D \cong 0.20$. Here the two points are above the albedo curve. A theoretical curve assuming isotropic scattering from the surface of the concrete is just like the cosine scattering curve of Fig. 13 except that it reaches its maximum for $h/D = 0.00$ instead of $h/D \cong 0.35$. Because of this, if a correction due to isotropic scattering were added to the cosine scattering curve, the theoretical curve would more nearly approach the experimental curve.

VI. CONCLUSION

The inverse square law predicts the approximate dose rate for source to detector spacings of twenty to one hundred and fifty centimeters. The neutron dose rate varies with the height of the detector and the source above a concrete slab, and with the distance between the source and detector. If a conical paraffin frustum long enough to reduce the direct beam by a factor of a few thousand is placed between the source and the detector with the small end against the source, the detector dose rate response is essentially that due to scattered neutrons. The results of this experiment apply directly to the case in which one wishes to calibrate a neutron dosimeter in air by weighting the neutron spectrum reaching the instrument using the first collision dose curve.

APPENDIX I

By means of the albedo theory[7] a theoretical equation can be formulated that predicts the neutron dose rate. Before the equation can be formulated there are several assumptions that must be made: a), the amount and angular distribution of the concrete re-radiated energy per unit of incident energy is assumed to be independent of the angle of the incident energy of the concrete; b), the amount of the re-radiated energy is assumed to be proportional to the cosine of the angle of the re-radiated energy with respect to the normal to the surface of the concrete; c), the concrete is assumed to re-radiate an amount of energy which is proportional to the amount of energy incident upon it (the proportionality constant is defined as the energy albedo α, i.e., the reflection coefficient); d), the extent of the source is assumed to be much less than D so that the source is effectively a point; and e), air attenuation of the neutrons is neglected.

Several symbols must be defined.

E_{cos} = the energy scattered from the concrete reaching the detector per square centimeter per second assuming cosine scattering.

N_o = the number of particles emitted from the source, isotropically, per second.

E_o = the energy of each particle.

From Fig. 14 the energy flux on the element ds of the reflecting surface is

$$\frac{E_o N_o}{4\pi r^2} \cdot \frac{h}{r}$$

UNCLASSIFIED
ORNL-LR-DWG. 10484

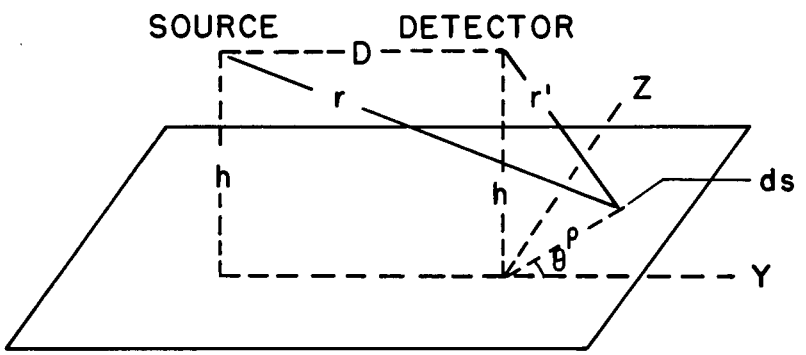

GEOMETRY FOR SCATTERING
FIGURE 14

The scattered energy flux from this element of area is

$$\alpha \cdot \frac{E_o N_o}{4\pi r^2} \cdot \frac{h}{r} \cdot ds \quad .$$

Now if we suppose that the back-scattered flux is proportional to the cosine law (Lambert's law), and if $\Delta\Omega = \pi r_1^2/r'^2$ (where r_1 is the radius of the detector) is the element of solid angle subtended by the receiver at the scattering point, the energy per second scattered to the receiver from ds is

$$\alpha \cdot \frac{E_o N_o}{4\pi r^2} \cdot \frac{h}{r} \cdot \frac{\Delta\Omega}{\pi} \cdot \frac{h}{r'} \cdot ds$$

The total energy scattered into the receiver per second per unit area of the receiver is thus

$$E_{cos} = \alpha \cdot \frac{E_o N_o}{4\pi} \cdot \frac{h^2}{\pi} \int\int_S \frac{ds}{r^3 r'^3}$$

Since

$$r^2 = \rho^2 + h^2, \quad \text{and } r'^2 = \rho^2 + 2D\rho \cos\theta + D^2 + h^2,$$

and if

$$E_{cos} = E_s \cdot F_1,$$

where

$$E_s = \frac{\alpha E_o N_o h^2}{4\pi^2}, \quad \text{and} \quad F_1 = \int\int_S \frac{ds}{r^3 r'^3},$$

then

$$F_1 = \int_0^{\infty} \int_0^{2\pi} \frac{\rho\, d\rho\, d\theta}{(\rho^2 + h^2)^{3/2} \quad (\rho^2 + 2D\rho \cos\theta + h^2 + D^2)^{3/2}}$$

From this follows

$$F_1 = \int_0^{\infty} \frac{\rho\, d\rho}{(\rho^2 + h^2)^{3/2}} \int_0^{2\pi} \frac{d\theta}{\left[(\rho + D)^2 + h^2 - 2D\rho(1 - \cos\theta)\right]^{3/2}}$$

$$F_1 = \int_0^{\infty} \frac{\rho\, d\rho}{(\rho^2 + h^2)^{3/2}} \int_0^{2\pi} \frac{d\theta}{\left(\left[(\rho + D)^2 + h^2\right]\left[1 - \frac{2D\rho(2)(1 - \cos\theta)}{([\rho + D]^2 + h^2)(2)}\right]\right)^{3/2}}$$

Let

$$K^2 = \frac{4D\rho}{(\rho + D)^2 + h^2} \qquad \text{where } K^2 < 1 ,$$

then,

$$F_1 = \int_0^{\infty} \frac{4\rho\, d\rho}{(\rho^2 + h^2)^{3/2} \left((\rho + D)^2 + h^2\right)^{3/2}} \int_0^{\pi/2} \frac{d\theta}{\left[1 - K^2\left(\frac{1 - \cos\theta}{2}\right)\right]^{3/2}}$$

$$F_1 = \int_0^{\infty} \frac{4\rho\, d\rho}{(\rho^2 + h^2)^{3/2} \left((\rho + D)^2 + h^2\right)^{3/2}} \int_0^{\pi/2} \frac{d\theta}{(1 - K^2 \sin^2 \theta/2)^{3/2}}$$

$$F_1 = \int_0^{\infty} \frac{4\rho\, d\rho}{(\rho^2 + h^2)^{3/2} \left((\rho + D)^2 + h^2\right)^{3/2}} \int_0^{\pi/2} (1 - K^2 \sin^2 \theta/2)^{-3/2}\, d\theta$$

If $(1 - K^2 \sin^2 \theta/2)^{-3/2}$ is expanded,

$$F_1 = \int_0^{\infty} \frac{4\rho\, d\rho}{(\rho^2 + h^2)^{3/2} \left((\rho + D)^2 + h^2\right)^{3/2}} \int_0^{\pi/2} d\theta \left[1 - 3/2\,(-K^2 \sin^2 \theta/2)\right.$$

$$\left. - \frac{3/2\,(-5/2)(-K^2 \sin^2 \theta/2)^2}{2\,!} - \frac{3/2\,(-5/2)(-7/2)(-K^2 \sin^2 \theta/2)^3}{3\,!} - - -\right]$$

Now rearranging and completing the steps,

$$F_1 = \int_0^{\infty} \frac{4\rho\, d\rho}{(\rho^2 + h^2)^{3/2} \left((\rho + D)^2 + h^2\right)^{3/2}} \int_0^{\pi/2} d\theta \left[1 + 3/2\, K^2 \sin^2 \theta/2\right.$$

$$\left. + \frac{3\cdot 5}{2\cdot 4} K^4 \sin^4 \theta/2 + \frac{3\cdot 5\cdot 7}{2\cdot 4\cdot 6} K^6 \sin^6 \theta/2 + - - - - -\right]$$

If we integrate from zero to $\pi/2$,

$$F_1 = \int_0^\infty \frac{4\rho d\rho}{(\rho^2 + h^2)^{3/2}\left((\rho + D)^2 + h^2\right)^{3/2}} \left[\pi/2 + 3/2\, K^2\, (1/2)(\pi/2)\right.$$

$$\left. + \left(\frac{3\cdot 5}{2\cdot 4}\right) K^4 \left(\frac{3}{2\cdot 4}\right)(\pi/2) + \left(\frac{3\cdot 5\cdot 7}{2\cdot 4\cdot 6}\right) K^6 \left(\frac{3\cdot 5}{2\cdot 4\cdot 6}\right)(\pi/2) + \text{--------}\right]$$

If this is rearranged into a more convenient form,

$$F_1 = \int_0^\infty \frac{4\rho d\rho}{(\rho^2 + h^2)^{3/2}\left((\rho + D)^2 + h^2\right)^{3/2}}\ \pi/2 \left[1 + 3/4\, K^2 + \frac{3\cdot 5}{2\cdot 4}\ K^4\right.$$

$$\left. \cdot\ \frac{3}{2\cdot 4} + \frac{3\cdot 5\cdot 7}{2\cdot 4\cdot 6}\ K^6\ \frac{3\cdot 5}{2\cdot 4\cdot 6} + \text{--------}\right]$$

Multiplying both numerator and denominator by $(1 - K^2)$,

$$F_1 = \int_0^\infty \frac{4\rho\, d\rho \;/\; (1 - K^2)}{(\rho^2 + h^2)^{3/2} \left((\rho + D)^2 + h^2\right)^{3/2}} \quad \frac{\pi}{2} \left[1 - K^2 + 3/4\, K^2 \right.$$

$$\left. - 3/4\, K^4 + \left(\frac{3\cdot 5}{2\cdot 4}\right) K^4 \left(\frac{3}{2\cdot 4}\right) - \left(\frac{3\cdot 5}{2\cdot 4}\right) K^6 \left(\frac{3}{2\cdot 4}\right) + \left(\frac{3\cdot 5\cdot 7}{2\cdot 4\cdot 6}\right) K^6 \left(\frac{3\cdot 5}{2\cdot 4\cdot 6}\right) - - - \right]$$

If the like terms are collected,

$$F_1 = \int_0^\infty \frac{4\rho\, d\rho \;/\; (1 - K^2)}{(\rho^2 + h^2)^{3/2} \left((\rho + D)^2 + h^2\right)^{3/2}} \quad \frac{\pi}{2} \left[1 - (1/2)^2 K^2 \right.$$

$$\left. - \left(\frac{3}{2\cdot 4}\right)^2 \frac{K^4}{3} - \left(\frac{3\cdot 5}{2\cdot 4\cdot 6}\right)^2 \frac{K^6}{5} - - - - - \right]$$

Now looking in the handbook,[8]

$$E(K, \pi/2) = \int_0^{\pi/2} \sqrt{1 - K^2 \sin^2 \psi}\; d\psi = \frac{\pi}{2} \left[1 - \left(\frac{1}{2}\right)^2 K^2 - \left(\frac{3}{2\cdot 4}\right)^2 \frac{K^4}{3} \right.$$

$$\left. - \left(\frac{3\cdot 5}{2\cdot 4\cdot 6}\right)^2 K^6/5 - - - - - \right]$$

---

8 Burington, R. S., Handbook of Mathematical Tables and Formulas (1949).

where $E(K, \pi/2)$ is a complete elliptic integral of the second kind. So,

$$F_1 = 4 \int_0^{\infty} \frac{\rho \, d\rho}{(\rho^2 + h^2)^{3/2} \left((\rho + D)^2 + h^2\right)^{3/2}} \cdot \frac{E(K, \pi/2)}{1 - K^2}$$

and finally,

$$E_{cos} = \frac{\alpha E_o N_o h^2}{4\pi^2} \left[4 \int_0^{\infty} \frac{\rho \, d\rho}{(\rho^2 + h^2)^{3/2} \left((\rho + D)^2 + h^2\right)^{3/2}} \cdot \frac{E(K, \pi/2)}{1 - K^2} \right] \quad (1).$$

Equation (2) is obtained from equation (1) by multiplying both numerator and denominator by $2D^2h^4$.

$$E_{cos} = \frac{\alpha E_o N_o}{8\pi^2 D^2} \left(\frac{D^2}{h^2}\right) \left[8h^4 \int_0^{\infty} \frac{\rho \, d\rho}{(\rho^2 + h^2)^{3/2} \left((\rho + D)^2 + h^2\right)^{3/2}} \cdot \frac{E(K, \pi/2)}{1 - K^2} \right] \quad (2)$$

If $k = D/h$

and if

$$f(k) = 8h^4 \int_0^{\infty} \frac{\rho \, d\rho}{(\rho^2 + h^2)^{3/2} \left((\rho + D)^2 + h^2\right)^{3/2}} \cdot \frac{E(K, \pi/2)}{1 - K^2} \tag{3}$$

then,

$$E_{cos} = \frac{\alpha E_o N_o k^2}{8\pi^2 D^2} f(k) . \tag{4}$$

A graph of f(k) vs k is shown in Fig. 15.[9]

$$\text{Ratio of Energy Rate} = \frac{\text{Energy}_{\text{total}}}{\text{Energy}_{\text{direct}}} = \frac{\text{Energy}_{\text{direct}} + \text{Energy}_{\text{scattered}}}{\text{Energy}_{\text{direct}}} \tag{5}$$

$$\text{Ratio of Energy Rate} = \frac{\dfrac{N_o E_o}{4\pi D^2} + \dfrac{\alpha E_o N_o k^2 f(k)}{8\pi^2 D^2}}{\dfrac{N_o E_o}{4\pi D^2}} = 1 + \frac{\alpha}{2\pi} k^2 f(k) \tag{6}$$

---

[9] This curve was originally given by M. S. Plesset, RAD-196, however, R. H. Ritchie of ORNL found that the curve was in error for large values of K. Fig. 15 is the curve as corrected by R. H. Ritchie.

UNCLASSIFIED
ORNL-LR DWG. 10486

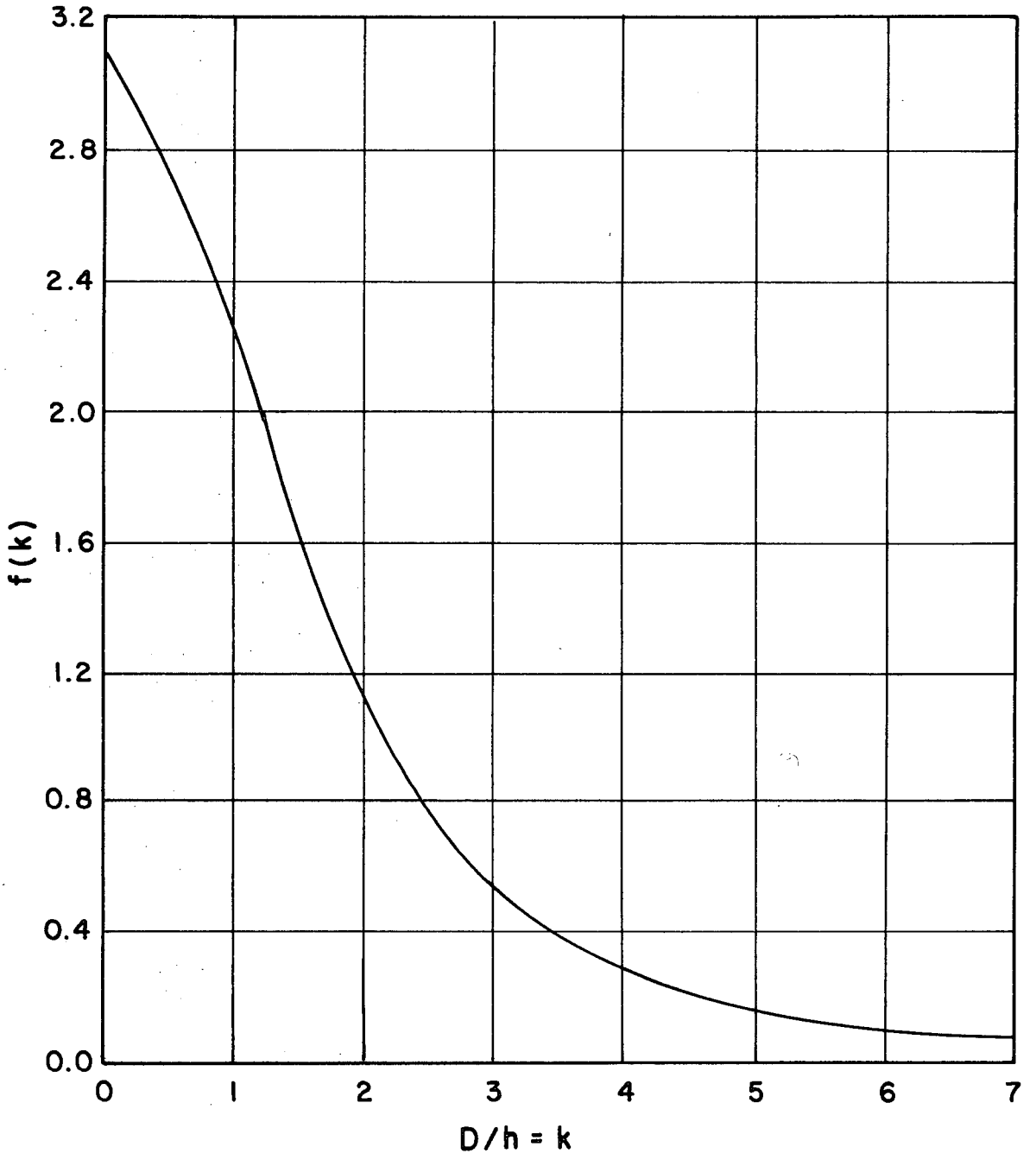

FIGURE 15

The neutron source is fairly monoenergetic,[5] and since dose is energy absorbed per unit volume, the dose rate would be proportional to the energy rate or

$$\text{Ratio of Dose Rate} = 1 + \frac{\alpha}{2\pi} k^2 f(k). \qquad (7)$$

In equation (7) α is the dose albedo instead of the energy albedo as originally defined.

BIBLIOGRAPHY

Barr, T. A., and Hurst, G. S., "Fast Neutron Dose in a Large Tissue-Equivalent Phantom," Nucleonics 12, No. 8, 33-35 (August 1954).

Burington, R. S., Handbook of Mathematical Tables and Formulas, Handbook Publishers, Inc. (1949).

Cochran, R. G., and Henry, K.M., "A Proton Recoil Type Fast-Neutron Spectrometer," ORNL-1479 (April 2, 1953).

Cure, J. W., and Hurst, G. S., "Fast Neutron Scattering - A Correction for Dosimetry," Nucleonics 12, No. 8, 36-38 (August 1954).

Glass, F. M., and Hurst, G. S., "A Method of Pulse Integration Using Binary Scaling Units," Rev. of Sci. Instr. 23, 67-72 (February 1952).

Hurst, G. S., "An Absolute Tissue Dosemeter for Fast Neutrons," Brit. J. Radiol. XXVII, No. 318, 353-357 (June 1954).

Hurst, G. S., and Ritchie, R. H., "Fast Neutron Dosimetry," Radiology 60, No. 6, 864-868 (June 1953).

Plesset, M. S., "Scattering of Gamma Rays and Neutrons," RAD-196 (August 29, 1948).